



## Article

**Cite this article:** Leung J, Hudson TS, Kendall JM, Barcheck G (2025) Evidence that seismic anisotropy captures upstream palaeo-ice fabric: Implications on present-day deformation at Whillans Ice Stream, Antarctica. *Journal of Glaciology* **71**, e39, 1–9. <https://doi.org/10.1017/jog.2025.19>

Received: 7 November 2023

Revised: 5 March 2025

Accepted: 5 March 2025

**Keywords:**

Ice streams; Seismology; Anisotropic ice

**Corresponding author:** Justin Leung;

Email: [justin.leung@earth.ox.ac.uk](mailto:justin.leung@earth.ox.ac.uk)

# Evidence that seismic anisotropy captures upstream palaeo-ice fabric: Implications on present-day deformation at Whillans Ice Stream, Antarctica

Justin Leung<sup>1</sup> , Thomas Samuel Hudson<sup>1,2</sup> , John-Michael Kendall<sup>1</sup>  and Grace Barcheck<sup>3</sup> 

<sup>1</sup>Department of Earth Sciences, University of Oxford, Oxford, UK; <sup>2</sup>Department of Earth and Planetary Sciences, ETH Zurich, Zürich, Switzerland and <sup>3</sup>Department of Earth and Atmospheric Sciences, Cornell University, Ithaca, NY, USA

**Abstract**

Understanding deformation and slip at ice streams, which are responsible for 90% of Antarctic ice loss, are vital for accurately modelling large-scale ice flow. Ice crystal orientation fabric (COF) has a first-order effect on ice stream deformation. For the first time, we use shear-wave splitting measurements of basal icequakes at Whillans Ice Stream (WIS), Antarctica, to determine a shear-wave anisotropy with an average delay time of 7 ms and fast S-wave polarisation ( $\varphi$ ) of 29.3°. The polarisation is expected to align perpendicular to ice flow, whereas our observation is oblique to the current ice flow direction ( $\sim 280^\circ$ ). This suggests that ice at WIS preserves upstream fabric caused by palaeo-deformation developed over at least the past 450 years, which provides evidence of the concept of microstructural fading memory. Our results imply that changes in the shape of WIS occur on timescales shorter than COF re-equilibration. The ‘palaeo-fabric’ can somewhat control present-day ice flow, which we suggest may somewhat contribute to the long-term slowdown at WIS. Our findings suggest that seismic anisotropy can provide information on past ice sheet dynamics, and how past ice dynamics can play a role in controlling current deformation.

**1. Introduction**

Despite ice streams spanning only 10% of Antarctica’s surface area, they are responsible for 90% of Antarctic ice loss (Morgan and others, 1982). Therefore, studying ice stream rheology is important for understanding Antarctica’s contribution to sea-level rise. One source of uncertainty in ice stream dynamics is the effect of ice fabrics on rheology, where ice with a crystal oriented fabric (COF) can be ten times weaker in shear in a particular direction relative to isotropic ice (Pimienta and others, 1987; Budd and Jacka, 1989). Glacial ice is formed of anisotropic grains with hexagonal crystalline symmetry, such that the viscosity along the basal plane of ice (normal to  $c$ -axis) is 60 times less than that perpendicular to it (Duval and others, 1983). Under stress, the  $c$ -axes in a bulk polycrystalline ice mass can rotate to form an ice COF over timescales of hundreds of years, which can change in response to the stress it encounters (Azuma, 1994). Hence, understanding ice COF provides insight on past deformation history and how it might influence future ice flow.

Most glacial ice COF measurements are taken from microstructural analyses of ice core samples. However, these are usually measured from stable or slow-moving regions of ice sheets and cannot provide much information of the physical processes in fast-deforming regions (Fan and others, 2021; Llorens and others, 2022). In contrast, seismic anisotropy measurements can be used to deduce ice COF properties over large areas in different ice settings, including ice streams (Smith and others, 2017). Therefore, seismic anisotropy can provide insight in these key fast-flowing regions, which can inform models of ice-sheet dynamics.

Whillans Ice Stream (WIS) is a major ice stream in West Antarctica that flows into the Ross Sea embayment (see Fig. 1; Picotti and others, 2015). The downstream portion of WIS is known as Whillans Ice Plain (WIP), and it flows at a speed of over 300 m per year, with stable sliding of the ice stream punctuated one to two times daily by sudden unstable sliding motion during 30 min slip events that also produce high frequency icequakes and tremor (Bindschadler and others, 2003; Winberry and others, 2013; Barcheck and others, 2018). Long-term slowdown of the ice stream can be seen, with longer periods of quiescence between slip events over time, suggesting possibility of future stagnation (Winberry and others, 2014). WIS is an excellent area to study basal seismicity given that seismic and global navigation satellite system data have been collected over recent decades at numerous

© The Author(s), 2025. Published by Cambridge University Press on behalf of International Glaciological Society. This is an Open Access article, distributed under the terms of the Creative Commons Attribution licence (<http://creativecommons.org/licenses/by/4.0>), which permits unrestricted re-use, distribution and reproduction, provided the original article is properly cited.

[cambridge.org/jog](https://www.cambridge.org/jog)

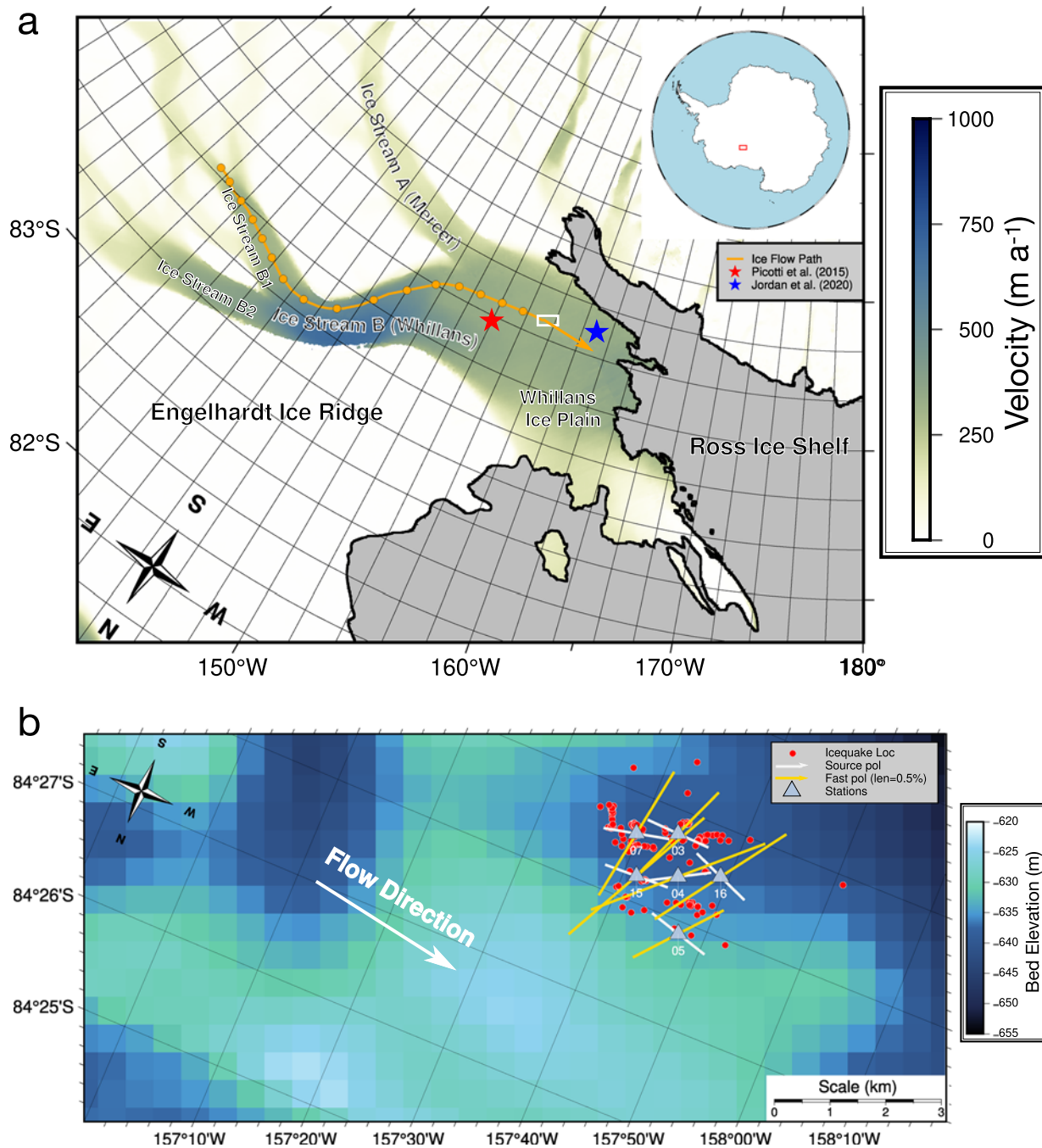


**Figure 1.** Stereographic maps showing Whillans Ice Stream (WIS) and study location. (a) Regional map of the WIS. The grounding line is marked in the thick black line, and the grey shaded areas mark regions of floating ice. The blue and red star show the study site locations of Jordan and others (2020) and Picotti and others (2015), respectively. The orange line outlines the upstream flow path of the ice at our study site location, assuming current flow velocities, with orange points marking the locations at intervals of 50 years (see supplementary information for flow path calculation). The background colour map shows the ice flow velocity obtained from MEaSURES InSAR-Based Antarctica Ice Velocity Map, Version 2 (Rignot and others, 2017). The study area in (b) is outlined by the white box. (b) Detailed map of the study region. Stations are marked as blue triangles, and icequake locations are shown by red scatter points. Gold lines show the fast S-wave polarisation direction, with the length of the line representing the strength of anisotropy. White lines show the source polarisations for each event, as estimated from recorded shear waves. Dominant ice flow direction (280°) is indicated by the large white arrow. The background colour map shows the bed elevation (Morlighem, 2022).

sites to study its stick-slip cycle (e.g. Winberry and others, 2009; Walter and others, 2011; Winberry and others, 2011; Pratt and others, 2014; Walter and others, 2015; Barcheck and others, 2020) and basal hydrologic cycle (e.g. Fricker and Scambos, 2009; Siegfried and others, 2016).

There are currently few ice COF observations for the entire ice column at WIS. Picotti and others (2015) used active

seismic sources to suggest an azimuth-independent vertically transverse isotropic fabric at WIS, with a focus on the top 200 m. Conversely, Jordan and others (2020) used electromagnetic methods to argue that the  $c$ -axes orient parallel to flow at WIS by polarimetric radar sounding that measured the top 400 m of WIS (see Fig. 1 for locations). Here, we provide the first seismic anisotropy measurements from shear-wave

splitting (SWS) of basal icequakes of the entire ice column at WIS.

## 2. Methodology

This study uses 319 icequakes recorded between 20 January and 27 February 2014 by six seismometers at WIP, Antarctica, part of a network active between 2012 and 2018 (Schwartz, 2012; Barcheck and others, 2020). The ice at the study site is between 690 and 710 m thick (Barcheck and others, 2020) and moving at  $\sim 370 \text{ m a}^{-1}$  (Morlighem, 2022). Since horizontal orientation of the instruments is important for studying seismic anisotropy, we verified the orientation of these instruments using a teleseismic event. We performed a manual search for icequakes focused within the duration of bidaily slip events at WIS, described in Barcheck and others (2021). Icequake arrival times are picked manually and are located using NonLinLoc, a probabilistic nonlinear earthquake location algorithm (Lomax and others, 2000). Only icequakes originating at the bed of the ice stream are of interest for measuring total anisotropy in the ice column; therefore, icequakes with a source depth shallower than 400 m are removed. Each icequake is filtered by a 10–100 Hz bandpass filter, based on the dominant source spectra of the icequakes (see Fig. S1). Seismic anisotropy is analysed on the horizontal (north and east) components because a  $\sim 100 \text{ m}$  thick firn layer refracts the ray path of icequakes to near-vertical incidence at the surface (Picotti and others, 2015).

SWS analysis is conducted using the python package SWSPy (Hudson and others, 2023), based on the approach of Wuestefeld and others (2010). It can be summarised as follows: First, a range of analysis time windows are defined because SWS measurements are sensitive to window lengths (Teaby and others, 2004). Second, a grid search is performed over fast shear-wave polarisation of  $-90^\circ < \varphi \leq 90^\circ$  and delay times between fast and slow S-waves of  $0 \leq \delta t \leq 0.1$  for each window, such that  $\varphi = 0$  represents a fast shear-wave polarisation in the north (and south) direction. The splitting parameters,  $\varphi$  and  $\delta t$ , associated with the minimum second eigenvalue of the S-wave covariance matrix that best linearise particle motion, describe the anisotropy observed along a given source-receiver ray path. Third, density-based cluster analysis is performed on all optimal  $\varphi$  and  $\delta t$  values, such that the optimal  $\varphi$  and  $\delta t$  values are obtained from the most stable cluster with minimum variance in  $\varphi$  and  $\delta t$  (Ester and others, 1996; Teaby and others, 2004). The source polarisation is then calculated by taking the azimuth of the largest eigenvalue of the covariance matrix of the linearised waveforms (Walsh and others, 2013).

A well-constrained result after SWS correction is defined as satisfying the following four requirements: (1) the particle motion (see Fig. 2c) becomes approximately linear after removing splitting using the optimal SWS parameters, (2) the error surface (see Fig. 2f) has a unique, well-constrained solution, (3) splitting parameters ( $\varphi$  and  $\delta t$ ) are stable (see Fig. 2e) throughout different clusters and (4) the quality factor  $Q_w$  is larger than 0.7.  $Q_w$  measures the robustness of the splitting measurement, and it is calculated by comparing the results from the eigenvalue method of Silver and Chan (1991) to the cross-correlation method of Menke and Levin (2003). A value of  $Q_w = 1$  signifies a perfect match between the two methods,  $Q_w = -1$  a good null result, and  $Q_w = 0$  a poor result (Wuestefeld and others, 2010).

The strength of anisotropy ( $\delta V$ ), or the difference between fast and slow S-wave velocities, can be quantified by the change in velocity, derived from the delay time ( $\delta t$ ):

$$\delta V = (V \times \delta t \times 100)/r, \quad (1)$$

where  $V = 1944 \text{ m s}^{-1}$  is the average isotropic shear-wave speed (Smith and others, 2017) and  $r$  the source-receiver distance.

## 3. Results

Eighty results from seventy events fulfil the aforementioned four criteria and, therefore, are chosen for further analysis. The fast S-wave polarisation  $\varphi$  and source polarisation of these events are plotted as polar histograms in Figure 3. For a double-couple icequake source associated with ice slip at the bed, S-wave source polarisation is aligned with the direction of slip (Hudson and others, 2020). One might typically expect the average S-wave source polarisation to align approximately with ice flow direction. Most source polarisation measurements lie approximately in the east–west direction with an average of  $264^\circ \text{ N} \pm 22^\circ$  (see Fig. 3a), which is in agreement with the WIS's flow direction of  $280^\circ \text{ N} \pm 2^\circ$  (Rignot and others, 2017).

The average delay time for these results is 7.1 ms and ranges from 1.6 ms to 19.2 ms. The average strength of anisotropy,  $\delta V$ , is  $\sim 1.5\%$ , with a maximum of 2.8%. This is below the maximum directional variation in S-wave velocities of single ice crystals of 12% (Lutz and others, 2020).

The SWS measurements have an overall mean fast S-wave direction ( $\varphi$ ) of  $29.3^\circ \text{ N} \pm 18^\circ$  (see Fig. 3b). The uncertainty in this result is defined as one standard deviation, likely representing an upper estimate of uncertainty in the result that could be caused by temporal variations in  $\varphi$  (see Fig. S2). Individual receivers generally have mean  $\varphi$  that fall within a range of  $22.4^\circ \text{ N}$ – $47.0^\circ \text{ N}$  (see Fig. 1b), with the exception of station WS07, which has a mean  $\varphi$  of  $9.1^\circ \text{ N}$  (see label 07, Fig. 1b). Ice core studies (Lipenkov and others, 1989; Wang and others, 2002; Weikusat and others, 2017) and seismic anisotropy studies (Smith and others, 2017; Kufner and others, 2023) have found that regions of longitudinal extension, such as ice divides and ice streams, have a vertical girdle fabric. In such fabrics,  $\varphi$  is found to be perpendicular to the ice flow direction (Harland and others, 2013). Based on ice flow direction derived from InSAR (Rignot and others, 2017) and the source polarisation data in Figure 3a, one would expect  $\varphi \sim 10^\circ \text{ N}$  at the Whillans study site (golden arrow, Fig. 3). However, the mean  $\varphi$  we observe of  $29.3^\circ \text{ N} \pm 18^\circ$  is oblique to this expected fast S-wave direction of  $\sim 10^\circ \text{ N}$ , even after accounting for uncertainty. A  $t$  test shows that the 95% confidence interval of the fast S-wave directions lies in between  $25.3^\circ \text{ N}$  and  $33.3^\circ \text{ N}$  (assuming that the distribution of fast S-wave directions in the data is Gaussian), confirming our confidence in this obliquity.

## 4. Discussion

### 4.1. Possible origins of an ice COF with an oblique fast S-wave direction

Our results suggest that the ice COF at WIS is oriented oblique, rather than perpendicular, to the ice flow direction. This obliqueness suggests one of two hypotheses: either that the local strain at our study site acts oblique to ice flow or that the ice COF at WIS is the result of preservation of historic deformation upstream of the study site.

Regarding the first hypothesis, a possible reason for extension oblique to ice flow is the differential ice flux between the two tributaries of WIP across a suture zone. The study site is located downstream of the confluence between the upper WIS and Mercer

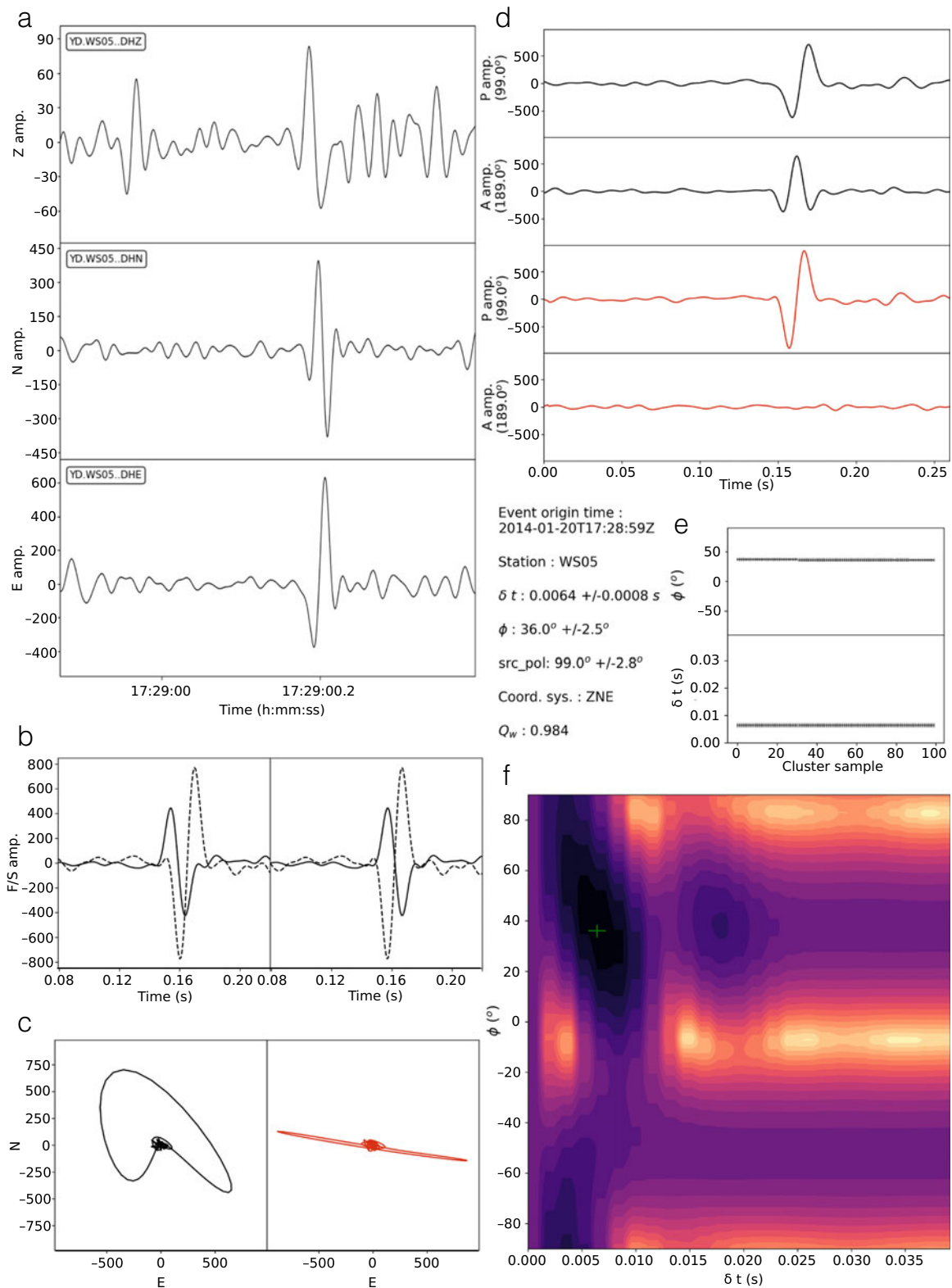


**Figure 2.** An example of a well-constrained shear-wave splitting event. (a) Icequake signal before correction in the vertical, north and east component. (b) The waveforms before (left) and after (right) SWS correction, plotted in the fast (black line) and slow (dotted) directions. (c) Horizontal (north and east) particle motion before (left) and after (right) SWS correction. (d) Particle motion of icequakes in the source polarisation (P) and the perpendicular azimuth (A) before (top two) and after (bottom two) correction. (e) Optimal  $\phi$  and  $\delta t$  for different cluster sizes. A good splitting measurement should have constant  $\phi$  and  $\delta t$  values independent of cluster size. (f) Error surface plotted on  $\phi$  vs  $\delta t$ . Larger errors are represented with brighter colours, and smaller errors with darker colours. The optimal  $\phi$  and  $\delta t$  and its uncertainties are shown with the green symbol.

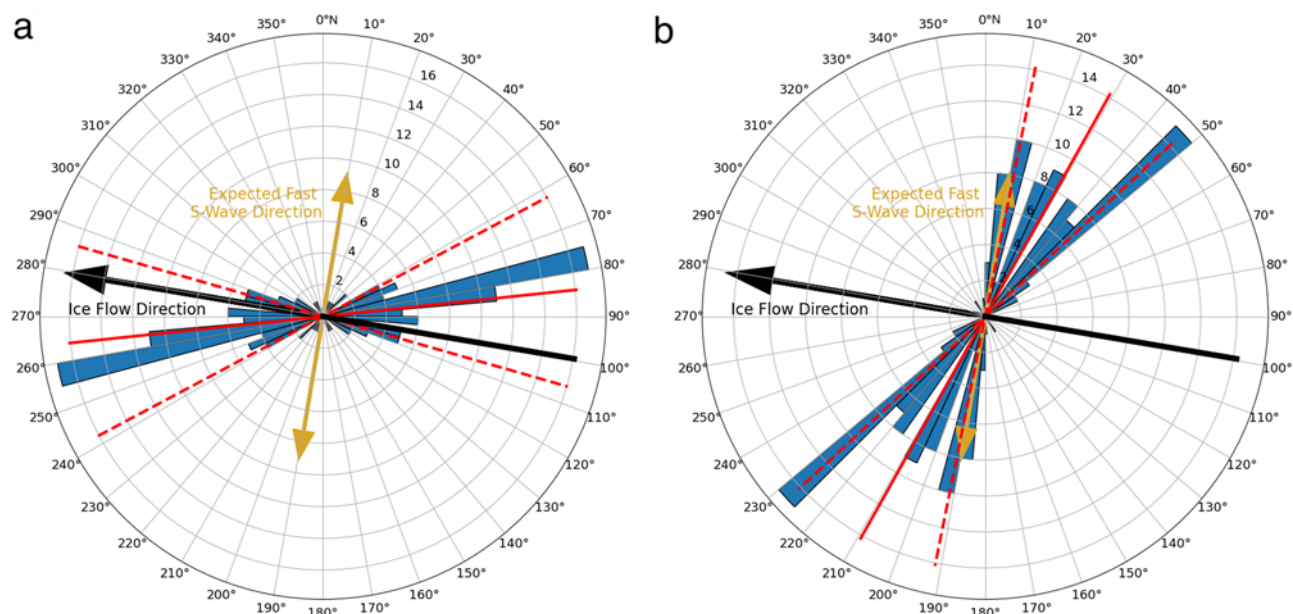


**Figure 3.** Rose diagrams of (a) source polarisations and (b) fast S-wave directions for all the 80 SWS measurements. The solid and dotted red lines indicate the averages and uncertainties respectively. The gold arrows on both diagrams indicate the expected fast S-wave direction based on ice flow direction, which are shown as black arrows (see main text for further details). Method for estimating uncertainty is included in the supplementary information.

Ice Stream (MIS), where the faster flow of WIS relative to MIS leads to shear strain across the suture zone, which can reorientate ice crystals (see Fig. 4; Beem and others, 2014). However, Bindshadler and others (1987) argue that shear is minimal between WIS and MIS. Additionally, we postulate that this suture zone has a negligible effect on the ice COF at our study site because the significant mixing between the two ice streams in the suture zone would perturb the ice fabric on length scales of the order of hundreds of metres. This mixing would likely yield significant differences in the fast-polarisation S-wave azimuth ( $\varphi$ ) between the different stations, yet the fast-polarisation S-wave azimuths remain constant within uncertainty across the network (see Fig. 1b) and a dominant fast polarisation direction can be seen in Figure 3b. Nonetheless, even if our ice COF were to be affected by this shearing, the suture zone is located upstream of our study site (see high strain rates near the intersection of WIS and MIS in Fig. 4) and therefore also supports the second hypothesis.

We instead favour the second hypothesis: that WIS has a ‘palaeo-COF’ that preserves a record of WIS upstream palaeo-deformation. Ice core studies and numerical simulations suggest that such preservation of a palaeo-COF is possible (Faria, 2018; Llorens and others, 2022). This can be explained by the concept of microstructural fading memory, where polycrystalline ice temporarily inherits signatures from its past microstructure that are progressively erased over a certain relaxation time (Faria, 2018). In the case of WIS, this past microstructure is the remnant of upstream palaeo-deformation, such that the COF still has not reoriented towards or re-equilibrated with the local principal compression direction. Most of the ice deformation at WIP occurs along the shear margins (Truffer and Echelmeyer, 2003) and ice flow is mainly accommodated by basal sliding, so internal deformation at Whillans is low but still existent. In such flow regimes, lattice rotation plays an important role relative to dynamic recrystallisation in ice fabric evolution (Azuma, 1994; Fan and others, 2021). The *c*-axes of the ice crystals always rotate

towards the principal direction of compression, which in ice streams is the azimuthal direction perpendicular to the flow direction (Thorsteinsson and others, 2003; Smith and others, 2017). The meandering nature of WIS alters the direction of compression, and therefore the ice COF, which we hypothesise in WIS evolves based on *c*-axis rotation, represents an integrated history of upstream strain induced by this changing stress. As such, it is difficult to pinpoint the origin of the fabric formation. However, for the ice COF to have developed the observed oblique  $\varphi$ , part of the integrated strain history must have originated from upstream areas in the ice stream where the flow direction was perpendicular to  $\varphi$ . Considering the present-day westward flow direction only and fast S-wave polarisation uncertainties of  $18^\circ$ , these regions have a flow direction approximately in the west–northwest direction of  $281^\circ\text{N}$ – $317^\circ\text{N}$  (see shaded red regions in Fig. 4). The nearest region with such a flow direction along the ice flow path is in the southern tributary of WIS, indicating that the ice COF could not have been purely derived from the integrated strain alone over the past 450 years. Consequently, this implies that the entire ice stream flow field of WIS changes on timescales shorter than ice COF re-equilibration. With this observation, we assumed constant flow directions with time because ice flow chronological studies do not suggest major changes in flow direction at WIS over the past 500 years (Catania and others, 2012). Furthermore, the validity of this assumption does not affect our conclusion of a palaeo-COF at WIS because present-day ice velocity orientations are insufficient to explain the observed  $\varphi$ .

Larger strain rates can accelerate the rotation of lattices, which reduces the re-equilibration timescales of ice fabrics and causes the COF to inherit signatures of the local strain field. Therefore, the integrated strain history better preserves the fabric along flow where the strain is greater. From present-day velocities, the largest strain rates are located on the main trunk of WIS before it merges with the MIS (see Fig. 4). However, these strain rates could have been different in the past because of the dynamic nature of ice

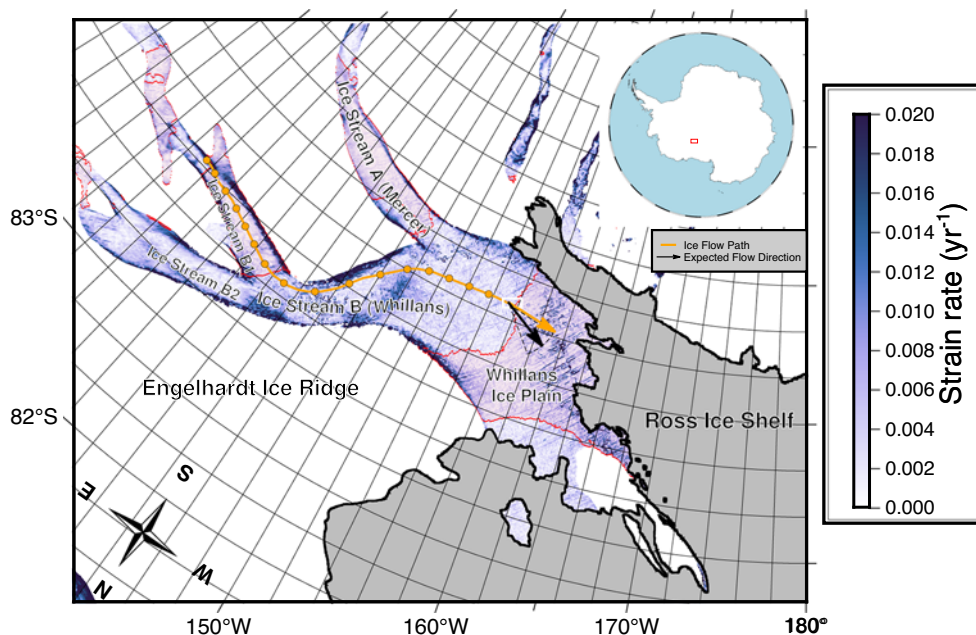


**Figure 4.** A summary of the study findings. Regions with a flow direction between  $281^\circ\text{N}$  and  $317^\circ\text{N}$  are shaded in red. The orange arrow shows the present-day flow direction. The black arrow indicates the flow direction inferred from the fast S-wave polarisation direction, and the dashed black sector outline shows the range of azimuths expressed by the red shaded regions. The background colour map is the strain rate calculated using the velocity map of Rignot and others (2017, supplementary information for calculation). Other features shown in this map are as in Figure 1a. The azimuth of the strain rate is shown in Figure S3.

streams. Some studies show that ice streams in the Ross Sea sector have variable mass fluxes over the past centuries, in particular the Kamb Ice Stream (Conway and others, 2002; Catania and others, 2012; Bougamont and others, 2015). Further studies of ice anisotropy, in combination with more detailed past ice conditions and flow calculations, would further evidence any dynamic changes in ice anisotropy along WIS.

Given that the expected  $\varphi$  based on current ice flow is only just outside the uncertainty of our results, we cannot ignore the possibility of an ice COF derived from the present-day study site. However, there is only a negligible part of the study area that has a flow direction between  $281^\circ\text{N}$  and  $317^\circ\text{N}$ , with the remainder of this region located downstream of the study site (see red shaded regions in Fig. 4). Hence, it is unlikely that enough time elapses for the ice COF to re-equilibrate with the present-day flow direction. We, therefore, suggest that the ice fabric is most likely derived from upstream palaeo-deformation.

#### 4.2. Comparison to other COF studies at WIS

Our results of an oblique fast S-wave direction ( $\varphi$ ) differ from previous findings of an azimuth-independent fabric (Picotti and others, 2015) and a fabric with  $\varphi$  parallel to flow between 170 m and 400 m depth (Jordan and others, 2020). We attribute these differences to variations in sampling location and depth (see Fig. 1a).

Jordan and others (2020) find two types of vertical girdle fabrics at different depths: a fabric with  $\varphi$  perpendicular to flow for ice up near the surface, and another fabric with  $\varphi$  parallel to flow up to 360 m deep. The former fabric agrees with our results, while the latter suggests a longitudinally compressive instead of longitudinally extensional stress regime, where compression and extension are defined as the principal compression axis being parallel and perpendicular to flow respectively. Because their study

was conducted near the grounding line (see Fig. 1a), we attribute the second girdle fabric ( $\varphi$  parallel to flow) to the influence of longitudinal compression due to stronger interactions between the ice and the bed topography near the grounding zone (Bindschadler and others, 1987; Picotti and others, 2015). If both fabrics are present in the ice column at our study site, because we only invert for a single anisotropic layer, both fabric orientations would then be represented as a single, composite result. If two perpendicular fabrics are present, then any SWS measurements would be unable to discriminate between the layers, with the anisotropy amplitude (delay-time) being damped or amplified, but the overall orientation of anisotropy remaining constant. Other studies have suggested that the stress regime at WIP is longitudinally compressive (Bindschadler and others, 1987). However, this likely does not apply to our study site. Firstly, the strain rates at WIS vary massively as little as 20 km (see fig. 9 of Bindschadler and others, 1987). Secondly, the ice flow path inferred from present-day velocities indicates that the ice at our study site has travelled along the outer part of the curve at WIP, where we expect the stress regime to be longitudinally extensional (see Fig. 4). Because most of the vertical shear needed to accommodate the driving stress at WIS occurs within the basal sediment layer (MacAyeal, 1989), we expect the velocity orientation to be similar across all depths of the ice stream. Thirdly, the ice at our study site is located sufficiently far from the grounding line, such that it should not experience significant longitudinal compression from interactions between the ice and grounding line bed topography (Pattyn, 2000).

Picotti and others (2015) observe an azimuth-independent fabric across the entire ice column and suggest that ice streams with low basal shear stress and highly water-saturated sediments have COF profiles similar to ice divides due to the increasing influence of vertical compression relative to transverse compression. However, most of their study is based on surface wave data and travel-time inversions that could only image the fabric up to 200 m

at WIS. Furthermore, their study site is located above Subglacial Lake Whillans, which is further inwards of the curve at WIP, where the stress regime is less longitudinally extensional (see Fig. 1a). Additionally, their ice COF is likely to have undergone more equilibration caused by higher strain rates and lower flow velocities on the northern side of WIS (see Fig. 4; Bindschadler and others, 1987). Given this variance in ice COF in WIS, future studies of ice deformation and anisotropy can furthermore reveal the spatial and temporal variability of ice COF at WIS.

#### 4.3. Comparison to other ice streams

SWS studies from another Antarctic ice stream, Rutford Ice Stream (RIS), find that the COF at RIS is approximately perpendicular ( $\sim 85^\circ$ ) to ice flow (Harland and others, 2013; Smith and others, 2017). Unlike the deviatoric nature of WIS stream flow, the flow direction at RIS is approximately linear over COF re-equilibration timescales. As such, it is not possible to discriminate to what extent the COF at RIS represents the current deformation or a preserved upstream deformation state. Kufner and others (2023) suggest that the RIS COF signal is dominated by the latter. The strength of anisotropy, effectively a measure of the strength of the ice COF, at RIS is 3–5%, while that at WIS is 1.5%, suggesting that internal deformation is lower at WIS than RIS. This is consistent with findings that ice flow at WIS is mainly accommodated by lateral shearing at the margins and basal sliding, where the vertical shear strain rates required to support the driving stress are mostly confined within a weak basal till layer, and not within the ice itself (Blankenship and others, 1986; MacAyeal, 1989; Truffer and Echelmeyer, 2003).

A recent seismic anisotropy study at RIS by Kufner and others (2023) suggested that multi-layer anisotropy can be present in ice streams, where the deepest third of the ice stream is thought to comprise an azimuthally isotropic cluster fabric caused by basal shearing (Azuma, 1994). However, the apparent absence of multiple fast S-wave phase arrivals in our data suggests that the effects of any multi-layer anisotropy at WIS are negligible, to which here we define multi-layer anisotropy as a type of depth-dependent anisotropy with sharper changes in anisotropic signatures with depth. Indeed we did not observe sufficient hints of multi-layer splitting to invert for multiple layers, even though such an inversion is possible at ice streams (Hudson and others, 2023). Inverting for a multi-layer anisotropic model at WIS would introduce additional parameters on layer thicknesses and fast polarisation directions, which could result in overfitting of the data, compared to a single depth-integrated anisotropy model.

Because most of the vertical shear at WIS is accommodated within the basal sediment layer (MacAyeal, 1989), we would expect the surface velocity direction to represent the orientation of maximum strain with depth, except perhaps for a thin (1–10s metres) basal shear layer near the ice-bed interface, which could vary somewhat in orientation over short length scales (10–100s metres) due to local bed topography variations. The depth of ice affected by shearing will either be too thin to be observed in seismic length-scales or too weak to affect the overall anisotropic signature of the ice stream (Blankenship and others, 1986; Bindschadler and others, 1987). Additionally, even if the shear zone were to exhibit strong anisotropy, the cluster fabric that would likely result is azimuthally isotropic and therefore has little effect on our results of a preferred *c*-axis azimuth. In summary, we, therefore, would expect the dominant anisotropy to be oriented relative to surface ice flow velocity.

#### 4.4. Implications of an oblique ice fabric on ice flow

The effective viscosity for compression and extension is higher along the basal plane. As seen in RIS, where the horizontal *c*-axis is oriented perpendicular to flow, the effective viscosity is higher along flow than across flow (Jordan and others, 2022; Kufner and others, 2023). This hardening along the flow direction, which is perpendicular to the *c*-axes and parallel to the basal plane, is thought to increase the viscosity by an order of magnitude relative to isotropic ice (Kufner and others, 2023). However, our results at WIS show a *c*-axis orientation that is not perpendicular but oblique to ice flow or equivalently a misalignment of the basal plane with the flow direction. Because the basal plane is associated with directions of highest effective viscosity, this misalignment implies that internal deformation will be resisted more at WIS if the *c*-axis direction re-equilibrates with the local principal stress direction. The internal deformation in WIS might be minimal today, but it may become important in the future. Firstly, the long-term slowdown in WIS has been associated with basal strengthening, especially in the upper portion of the ice stream (Beem and others, 2014). If the driving stress is somehow sustained, then a lower proportion of this stress could be accommodated by the basal till and a higher proportion through internal deformation. Secondly, the deceleration results in increased duration between periods of slip events at WIS, which is expected to increase the significance of internal viscous deformation (Winberry and others, 2014).

Our observations also suggest that palaeo-ice COF can somewhat control present-day ice flow. If the shape of an ice stream deviates on length scales less than the distance ice travels within the COF re-equilibration time, then the COF may not be aligned with ice flow, limiting the effective viscosity of the ice column along the ice flow direction. If an ice stream flows linearly for a duration greater than the re-equilibration time, then the COF should re-equilibrate with the bulk stress, such that the basal plane will rotate closer to the ice flow direction, increase the effective viscosity and decrease the rate of deformation downstream. The degree of re-equilibration of an ice COF with the surrounding stresses is not only dependent on ice stream shape but also on flow speed. Slower-flowing ice will have more time to re-equilibrate with the surrounding stress field. The long-term slowdown at WIS can, therefore, provide more time for its ice COF re-equilibration, which reduces the misalignment of the basal plane with flow direction and increases the effective viscosity along the flow direction of WIS. Despite internal deformation becoming more significant with the long-term slowdown, this higher effective viscosity instead indicates that internal deformation will be more difficult, which has consequences on future predictions of the ice flow at WIS.

Most icesheet-scale ice dynamics models assume either that ice is isotropic or parameterise anisotropy effects via an enhancement factor to account for ice weakening due to COF orientation relative to ice flow. However, recent studies such as Smith and others (2017) and Kufner and others (2023) suggest that enhancement factors should no longer be used to parameterise ice viscosity in fast-deforming regions such as ice streams. Additionally, the effect of anisotropy on the viscosity of ice can differ significantly between different types of ice fabrics. Most results concluding that ice weakens when anisotropy is considered originate from studies based on cluster fabrics. Conversely, radar and seismic observations at RIS (Jordan and others, 2022; Kufner and others, 2023) and numerical simulations (Ma and others, 2010) show that ice with a girdle COF has a higher effective viscosity in relation to isotropic ice. Our findings at WIS further support the importance of characterising

COF- and directionally dependent ice viscosity in ice flow models and emphasise that understanding ice COF in both space and time is important for producing more realistic deformation in ice dynamics models.

## 5. Conclusion

This study provides SWS observations from basal icequakes at WIS. From these observations, we infer the ice COF anisotropy over the entire ice column. The observations provide insight into past and present deformation at WIS. The results from 80 discrete icequakes SWS observations show that WIS has an average fast S-wave direction ( $\varphi$ ) of  $29.3^\circ$ , which is oblique to the expected direction of  $\sim 10^\circ$  based on ice flow direction at the study site of around  $280^\circ$ . We suggest that the ice COF records an integrated strain history along its flow path for at least the past 450 years to have preserved deformation in the direction of  $\varphi$  and, therefore, evidence the concept of microstructural fading memory. The non-perpendicularity of  $\varphi$  to ice flow implies that the shape of an ice stream can affect its flow, such that spatially deviatoric ice streams including WIS can flow slower if they were instead linear. Given the long-term slowdown of WIS, the basal plane will have more time to re-equilibrate with the surrounding stress field, which can further contribute to the long-term slowdown. Our results have implications for ice sheet models, suggesting that historic ice flow can preserve ice fabric and hence directionally dependent ice viscosity that might play an important role in such models.

**Supplementary material.** The supplementary material for this article can be found at <https://doi.org/10.1017/jog.2025.19>.

**Acknowledgements.** J.L. received funding from a NERC DTP Award (NE/S007474/1). T.S.H. was funded by a Leverhulme Early Career Fellowship (ECF-2022-499). We thank Alex Brisbourne for his comments, which have improved the manuscript. For the purpose of Open Access, the authors have applied a CC BY public copyright licence to any Author Accepted Manuscript (AAM) version arising from this submission.

## References

- Azuma N (1994) A flow law for anisotropic ice and its application to ice sheets. *Earth and Planetary Science Letters* **128**, 601–614. doi: [10.1016/0012-821X\(94\)90173-2](https://doi.org/10.1016/0012-821X(94)90173-2)
- Barcheck CG, Schwartz SY and Tulaczyk S (2020) Icequake streaks linked to potential mega-scale glacial lineations beneath an Antarctic ice stream. *Geology* **48**, 99–102. doi: [10.1130/G46626.1](https://doi.org/10.1130/G46626.1)
- Barcheck CG, Tulaczyk S, Schwartz SY, Walter JI and Winberry JP (2018) Implications of basal micro-earthquakes and tremor for ice stream mechanics: Stick-slip basal sliding and till erosion. *Earth and Planetary Science Letters* **486**, 54–60. doi: [10.1016/j.jplgl.2017.12.046](https://doi.org/10.1016/j.jplgl.2017.12.046)
- Barcheck G, Brodsky EE, Fulton PM, King MA, Siegfried MR and Tulaczyk S (2021) Migratory earthquake precursors are dominant on an ice stream fault. *Science Advances* **7**, eabd0105. doi: [10.1126/sciadv.abd0105](https://doi.org/10.1126/sciadv.abd0105)
- Beem LH, Tulaczyk SM, King MA, Bougamont M, Fricker HA, and Christoffersen P (2014) Variable deceleration of Whillans Ice Stream, West Antarctica. *Journal of Geophysical Research: Earth Surface* **119**, 212–224. doi: [10.1002/2013JF002958](https://doi.org/10.1002/2013JF002958)
- Bindschadler RA, King MA, Alley RB, Anandakrishnan S and Padman L (2003) Tidally controlled stick-slip discharge of a West Antarctic ice stream. *Science* **301**, 1087–1089. <https://www.jstor.org/stable/3834979>
- Bindschadler RA, Stephenson SN, MacAyeal DR and Shabtaie S (1987) Ice dynamics at the mouth of Ice Stream B, Antarctica. *Journal of Geophysical Research* **92**, 8885. doi: [10.1029/JB092iB09p08885](https://doi.org/10.1029/JB092iB09p08885)
- Blankenship DD, Bentley CR, Rooney ST and Alley RB (1986) Seismic measurements reveal a saturated porous layer beneath an active Antarctic ice stream. *Nature* **322**, 54–57. doi: [10.1038/322054a0](https://doi.org/10.1038/322054a0)
- Bougamont M, Christoffersen P, Price SF, Fricker HA, Tulaczyk S and Carter SP (2015) Reactivation of Kamb Ice Stream tributaries triggers century-scale reorganization of Siple Coast ice flow in West Antarctica. *Geophysical Research Letters* **42**, 8471–8480. doi: [10.1002/2015GL065782](https://doi.org/10.1002/2015GL065782)
- Budd W and Jacka T (1989) A review of ice rheology for ice sheet modelling. *Cold Regions Science and Technology* **16**, 107–144. doi: [10.1016/0165-232X\(89\)90014-1](https://doi.org/10.1016/0165-232X(89)90014-1)
- Catania G, Hulbe C, Conway H, Scambos T and Raymond C (2012) Variability in the mass flux of the Ross ice streams, West Antarctica, over the last millennium. *Journal of Glaciology* **58**, 741–752. doi: [10.3189/2012JoG11J219](https://doi.org/10.3189/2012JoG11J219)
- Conway H, Catania G, Raymond CF, Gades AM, Scambos TA and Engelhardt H (2002) Switch of flow direction in an Antarctic ice stream. *Nature* **419**, 465–467. doi: [10.1038/nature01081](https://doi.org/10.1038/nature01081)
- Duval P, Ashby MF and Anderman I (1983) Rate-controlling processes in the creep of polycrystalline ice. *Journal of Physical Chemistry* **87**, 4066–4074. doi: [10.1021/j100244a014](https://doi.org/10.1021/j100244a014)
- Ester M, Kriegel HP, Sander J and Xu X (1996) A density-based algorithm for discovering clusters in large spatial databases with noise. In *Proceedings of the Second International Conference on Knowledge Discovery and Data Mining, KDD'96*. AAAI Press, Portland, Oregon, pp. 226–231.
- Fan S, Cross AJ, Prior DJ, Goldsby DL, Hager TF, Negrini M and Qi C (2021) Crystallographic preferred orientation (CPO) development governs strain weakening in ice: Insights from high-temperature deformation experiments. *Journal of Geophysical Research: Solid Earth* **126**, e2021JB023173. doi: [10.1029/2021JB023173](https://doi.org/10.1029/2021JB023173)
- Faria SH (2018) Slip-band distributions and microstructural fading memory beneath the firn-ice transition of polar ice sheets. *Mechanics Research Communications* **94**, 95–101. doi: [10.1016/j.mechrescom.2018.09.009](https://doi.org/10.1016/j.mechrescom.2018.09.009)
- Fricker HA and Scambos T (2009) Connected subglacial lake activity on lower Mercer and Whillans Ice Streams, West Antarctica, 2003–2008. *Journal of Glaciology* **55**, 303–315. doi: [10.3189/002214309788608813](https://doi.org/10.3189/002214309788608813)
- Harland S and 7 others (2013) Deformation in Rutford Ice Stream, West Antarctica: Measuring shear-wave anisotropy from icequakes. *Annals of Glaciology* **54**, 105–114. doi: [10.3189/2013AoG64A033](https://doi.org/10.3189/2013AoG64A033)
- Hudson TS, Asplet J and Walker AM (2023) Automated shear-wave splitting analysis for single- and multi-layer anisotropic media. *Seismica* **2**, doi: [10.26443/seismica.v2i2.1031](https://doi.org/10.26443/seismica.v2i2.1031)
- Hudson TS, Brisbourne AM, Walter F, Gräff D, White RS and Smith AM (2020) Icequake source mechanisms for studying glacial sliding. *Journal of Geophysical Research: Earth Surface* **125**, e2020JF005627. doi: [10.1029/2020JF005627](https://doi.org/10.1029/2020JF005627)
- Jordan TM, Martin C, Brisbourne AM, Schroeder DM and Smith AM (2022) Radar characterization of ice crystal orientation fabric and anisotropic viscosity within an Antarctic ice stream. *Journal of Geophysical Research: Earth Surface* **127**, e2022JF006673. doi: [10.1029/2022JF006673](https://doi.org/10.1029/2022JF006673)
- Jordan TM, Schroeder DM, Elsworth CW and Siegfried MR (2020) Estimation of ice fabric within Whillans Ice Stream using polarimetric phase-sensitive radar sounding. *Annals of Glaciology* **61**, 74–83. doi: [10.1017/aog.2020.6](https://doi.org/10.1017/aog.2020.6)
- Kufner S and 6 others (2023) Strongly depth-dependent ice fabric in a fast-flowing Antarctic ice stream revealed with icequake observations. *Journal of Geophysical Research: Earth Surface* **128**, e2022JF006853. doi: [10.1029/2022JF006853](https://doi.org/10.1029/2022JF006853)
- Lipenkov V, Barkov N, Duval P and Pimienta P (1989) Crystalline texture of the 2083 m ice core at Vostok Station, Antarctica. *Journal of Glaciology* **35**, 392–398. doi: [10.3189/S002214300009321](https://doi.org/10.3189/S002214300009321)
- Llorens MG and 9 others (2022) Can changes in deformation regimes be inferred from crystallographic preferred orientations in polar ice? *The Cryosphere* **16**, 2009–2024. doi: [10.5194/tc-16-2009-2022](https://doi.org/10.5194/tc-16-2009-2022)
- Lomax A, Virieux J, Volant P and Berge-Thierry C (2000) Probabilistic earthquake location in 3D and layered models. In CH Thurber and N Rabinowitz (eds.), *Advances in Seismic Event Location*. Springer, Netherlands, Dordrecht, pp. 101–134. doi: [10.1007/978-94-015-9536-0\\_5](https://doi.org/10.1007/978-94-015-9536-0_5)
- Lutz F and 9 others (2020) Constraining ice shelf anisotropy using shear wave splitting measurements from active-source borehole seismics. *Journal*

- of *Geophysical Research: Earth Surface* **125**, e2020JF005707. doi: [10.1029/2020JF005707](https://doi.org/10.1029/2020JF005707)
- Ma Y, Gagliardini O, Ritz C, Gillet-Chaulet F, Durand G and Montagnat M** (2010) Enhancement factors for grounded ice and ice shelves inferred from an anisotropic ice-flow model. *Journal of Glaciology* **56**, 805–812. doi: [10.3189/002214310794457209](https://doi.org/10.3189/002214310794457209)
- MacAyeal DR** (1989) Large-scale ice flow over a viscous basal sediment: Theory and application to ice stream B, Antarctica. *Journal of Geophysical Research* **94**, 4071–4087. doi: [10.1029/JB094iB04p04071](https://doi.org/10.1029/JB094iB04p04071)
- Menke W and Levin V** (2003) The cross-convolution method for interpreting SKS splitting observations, with application to one and two-layer anisotropic earth models. *Geophysical Journal International* **154**, 379–392. doi: [10.1046/j.1365-246X.2003.01937.x](https://doi.org/10.1046/j.1365-246X.2003.01937.x)
- Morgan V, Jacka T, Akerman G and Clarke A** (1982) Outlet glacier and mass-budget studies in Enderby, Kemp, and Mac. Robertson Lands, Antarctica. *Annals of Glaciology* **3**, 204–210. doi: [10.3189/S0260305500002780](https://doi.org/10.3189/S0260305500002780)
- Morlighem M** (2022) *MEaSURES BedMachine Antarctica*. (NSIDC-0756, Version 3). [Data Set]. NASA National Snow and Ice Data Center Distributed Active Archive Center. doi: [10.5067/FPSU0V1MWUB6](https://doi.org/10.5067/FPSU0V1MWUB6)
- Pattyn F** (2000) Ice-sheet modelling at different spatial resolutions: Focus on the grounding zone. *Annals of Glaciology* **31**, 211–216. doi: [10.3189/172756400781820435](https://doi.org/10.3189/172756400781820435)
- Picotti S, Vuan A, Carcione JM, Horgan HJ and Anandakrishnan S** (2015) Anisotropy and crystalline fabric of Whillans Ice Stream (West Antarctica) inferred from multicomponent seismic data. *Journal of Geophysical Research: Solid Earth* **120**, 4237–4262. doi: [10.1002/2014JB011591](https://doi.org/10.1002/2014JB011591)
- Pimienta P, Duval P and Lipenkov VY** (1987) Mechanical behavior of anisotropic polar ice. The physical basis of ice sheet modelling. 9–22 August 1987 Vancouver, Canada. In *Proceedings of the Vancouver Symposium*. International Association of Hydrological Sciences, Vol. 170, pp. 57–66.
- Pratt MJ, Winberry JP, Wiens DA, Anandakrishnan S and Alley RB** (2014) Seismic and geodetic evidence for grounding-line control of Whillans Ice Stream stick-slip events. *Journal of Geophysical Research: Earth Surface* **119**, 333–348. doi: [10.1002/2013JF002842](https://doi.org/10.1002/2013JF002842)
- Rignot E, Mouginot J, Morlighem M and Scheuchl B** (2017) *MEaSURES InSAR-Based Antarctica Ice Velocity Map*. (NSIDC-0484, Version 2). [Data Set]. NASA National Snow and Ice Data Center Distributed Active Archive Center. doi: [10.5067/D7GK8F5J8M8R](https://doi.org/10.5067/D7GK8F5J8M8R)
- Schwartz SY** (2012) *Whillans Ice Stream Subglacial Access Research Drilling* [Data set]. International Federation of Digital Seismograph Networks. doi: [10.7914/SN/YD\\_2012](https://doi.org/10.7914/SN/YD_2012)
- Siegfried MR, Fricker HA, Carter SP and Tulaczyk S** (2016) Episodic ice velocity fluctuations triggered by a subglacial flood in West Antarctica. *Geophysical Research Letters* **43**, 2640–2648. doi: [10.1002/2016GL067758](https://doi.org/10.1002/2016GL067758)
- Silver PG and Chan WW** (1991) Shear wave splitting and subcontinental mantle deformation. *Journal of Geophysical Research*, 96(B10), 16429–16454. doi: [10.1029/91JB00899](https://doi.org/10.1029/91JB00899)
- Smith EC and 6 others** (2017) Ice fabric in an Antarctic ice stream interpreted from seismic anisotropy. *Geophysical Research Letters* **44**, 3710–3718. doi: [10.1002/2016GL072093](https://doi.org/10.1002/2016GL072093)
- Teanby NA and 6 others** (2004) Automation of shear-wave splitting measurements using cluster analysis. *Bulletin of the Seismological Society of America* **94**, 453–463. doi: [10.1785/0120030123](https://doi.org/10.1785/0120030123)
- Thorsteinsson T, Waddington ED and Fletcher RC** (2003) Spatial and temporal scales of anisotropic effects in ice-sheet flow. *Annals of Glaciology* **37**, 40–48. doi: [10.3189/172756403781815429](https://doi.org/10.3189/172756403781815429)
- Truffer M and Echelmeyer KA** (2003) Of isbræ and ice streams. *Annals of Glaciology* **36**, 66–72. doi: [10.3189/172756403781816347](https://doi.org/10.3189/172756403781816347)
- Walsh E, Arnold R and Savage MK** (2013) Silver and Chan revisited. *Journal of Geophysical Research: Solid Earth* **118**, 5500–5515. doi: [10.1002/jgrb.50386](https://doi.org/10.1002/jgrb.50386)
- Walter JI, Brodsky EE, Tulaczyk S, Schwartz SY and Pettersson R** (2011) Transient slip events from near-field seismic and geodetic data on a glacier fault, Whillans Ice Plain, West Antarctica. *Journal of Geophysical Research* **116**, F01021. doi: [10.1029/2010JF001754](https://doi.org/10.1029/2010JF001754)
- Walter JI, Svetlizky I, Fineberg J, Brodsky EE, Tulaczyk S, Grace Barcheck C and Carter SP** (2015) Rupture speed dependence on initial stress profiles: Insights from glacier and laboratory stick-slip. *Earth and Planetary Science Letters* **411**, 112–120. doi: [10.1016/j.jpl.2014.11.025](https://doi.org/10.1016/j.jpl.2014.11.025)
- Wang Y, Thorsteinsson T, Kipfstuhl J, Miller H, Dahl-Jensen D and Shoji H** (2002) A vertical girdle fabric in the NorthGRIP deep ice core, North Greenland. *Annals of Glaciology* **35**, 515–520. doi: [10.3189/172756402781817301](https://doi.org/10.3189/172756402781817301)
- Weikusat I and 10 others** (2017) Physical analysis of an Antarctic ice core-towards an integration of micro- and macrodynamics of polar ice. *Philosophical Transactions of the Royal Society A* **375**, 20150347. doi: [10.1098/rsta.2015.0347](https://doi.org/10.1098/rsta.2015.0347)
- Winberry JP, Anandakrishnan S, Alley RB, Bindschadler RA and King MA** (2009) Basal mechanics of ice streams: Insights from the stick-slip motion of Whillans Ice Stream, West Antarctica. *Journal of Geophysical Research* **114**, F01016. doi: [10.1029/2008JF001035](https://doi.org/10.1029/2008JF001035)
- Winberry JP, Anandakrishnan S, Alley RB, Wiens DA and Pratt MJ** (2014) Tidal pacing, skipped slips and the slowdown of Whillans Ice Stream, Antarctica. *Journal of Glaciology* **60**, 795–807. doi: [10.3189/2014JoG14J038](https://doi.org/10.3189/2014JoG14J038)
- Winberry JP, Anandakrishnan S, Wiens DA and Alley RB** (2013) Nucleation and seismic tremor associated with the glacial earthquakes of Whillans Ice Stream, Antarctica. *Geophysical Research Letters* **40**, 312–315. doi: [10.1002/grl.50130](https://doi.org/10.1002/grl.50130)
- Winberry JP, Anandakrishnan S, Wiens DA, Alley RB and Christianson K** (2011) Dynamics of stick-slip motion, Whillans Ice Stream, Antarctica. *Earth and Planetary Science Letters* **305**, 283–289. doi: [10.1016/j.jpl.2011.02.052](https://doi.org/10.1016/j.jpl.2011.02.052)
- Wuestefeld A, Al-Harrasi O, Verdon JP, Wookey J and Kendall JM** (2010) A strategy for automated analysis of passive microseismic data to image seismic anisotropy and fracture characteristics: A strategy for automated analysis of passive microseismic data. *Geophysical Prospecting* **58**, 755–773. doi: [10.1111/j.1365-2478.2010.00891.x](https://doi.org/10.1111/j.1365-2478.2010.00891.x)